UNIVERSITY OF WISCONSIN LA CROSSE

Graduate Studies

NUCLEAR LOCALIZATION AND NUCLEAR EXPORT SIGNALS OF THE HUMAN PARAINFLUENZA VIRUS MATRIX PROTEIN AND THEIR INVOLVEMENT IN NUCLEAR TRANSIT AND VIRUS RELEASE

A Manuscript Style Thesis Submitted in Partial Fulfillment of the Requirements for the Degree of Master of Science

Micaela Haas

College of Health and Science

Microbiology

May, 2018

NUCLEAR LOCALIZATION AND NUCLEAR EXPORT SIGNALS OF THE HUMAN PARAINFLUENZA VIRUS MATRIX PROTEIN AND THEIR INVOLVEMENT IN NUCLEAR TRANSIT AND VIRUS RELEASE

By Micaela Haas

We recommend acceptance of this thesis in partial fulfillment of the candidate's requirements for the degree of Master of Science in Microbiology

The candidate has completed the oral defense of the thesis.

Michael Hoffman, Ph.D. — 7/2/18 — Date

Thesis Committee Chairperson

Scott Cooper, Ph.D. — 6/28/2018 — Date

Thesis Committee Member

Peter Wilker, Ph.D. — 6/28/2018 — Date

Thesis Committee Member

Anton Sanderfoot, Ph.D. — 6/28/2018 — Date

Thesis Committee Member

Thesis accepted

Meredith Thomsen, Ph.D. — 7-2-18 — Date

Graduate Studies Director

ABSTRACT

Haas, M.H. Nuclear localization and nuclear export signals of the human parainfluenza virus matrix protein and their involvement in virus release. MS in Microbiology, May 2018, 47 pp. (M. Hoffman)

Matrix proteins of some viruses within the *Paramyxovirinae* subfamily transit through the nucleus. This process is needed for virus particle release from cells and is controlled by nuclear localization (NLS) and nuclear export signals (NES). This investigation sought to determine if the matrix protein of one paramyxovirus, human parainfluenza virus 3 (HPIV3) also transits through the nucleus in an NLS/NES-dependent manner. Toward this goal, wild-type and NLS/NES-mutated HPIV3 matrix proteins were expressed in 293T cells and immunofluorescent localization assays and virus-like particle (VLP) release assays were conducted. The wild-type matrix protein did localize to the nucleus and localization was influenced by NLS and NES mutations. The NLS mutant, K258A, limited entry of the matrix protein into the nucleus, and the NLS mutant, K258R, and the NES mutant, L106/107A, restricted release of the matrix protein from the nucleus. Regarding production of virus-like-particles, the wild-type M directed VLP formation but the NLS mutations limited formation. Expression of the L106/107A mutant was not detected, so VLP formation ability could not be determined. These results show that HPIV3 M protein nuclear transit was controlled by the NLS and NES signals and the lack of nuclear transit resulted in decreased VLP budding.

ACKNOWLEDGEMENTS

First, I would like to thank my thesis advisor, Michael Hoffman, PhD, who provided knowledge and guidance throughout my graduate studies. I also want to thank my thesis committee members Scott Cooper, PhD, Anton Sanderfoot, PhD, and Peter Wilker, PhD, for providing feedback, guidance, and suggestions. Additionally, I would like to thank Shanna Mueller for being willing to show me how to do any new technique in the lab that I was not familiar with and for being a great lab mate. I also would like to thank Brandon Harris for helping me with ImageJ and confocal microscopy. Additionally, I would like to thank the University of Wisconsin La Crosse Research, Service, Education, and Leadership (RSEL) grant for helping to fund my graduate research. Finally, I would like to thank my parents for their constant love, support, and encouragement.

TABLE OF CONTENTS

PAGE

LIST OF FIGURES

FIGURE PAGE

INTRODUCTION

Background

Human parainfluenza viruses (HPIVs) are non-segmented, negative sense RNA viruses in the *Paramyxoviridae* family of the *Mononegavirales* order. The *Mononegavirales* order has many different viruses that cause asymptomatic to life threatening diseases in both humans and animals. Other families within the *Mononegavirales* order include *Filoviridae*, *Rhabdoviridae*, *Nyamivardae*, and *Bornaviridae*. Members of the *Filoviridae* family are known to produce hemorrhagic fever; a prominent virus in this family is Ebola (EbV) (1). The *Rhabdoviridae* family contains the zoonotic virus rabies (2). The *Paramyxoviridae* family is divided into two subfamilies, the *Paramyxovirinae* and the *Pneumovirinae,* which are classified into seven genera. The *Paramyxovirinae* contains not only the four different types of HPIVs but also viruses such as mumps (MuV), measles (MeV), and Sendai virus (SeV) (3). HPIV3 belongs to the *Respirovirus* genus, along with HPV1, SeV, and bovine parainfluenza virus type 3 (bPIV3). All viruses in this genus cause respiratory infections to their hosts. SeV is the prototypic virus of not just the genus, but the entire family, and it primarily targets mice (4-8).

Clinical Significance

Since the late 1950s HPIVs have been classified into four different types serologically. HPIV1, 2, and 3 are the most common, and HPIV4 is the least prevalent. All HPIVs cause respiratory problems in humans. HPIV3 can spread through large

droplets or coming in contact with a contaminated surface (4,9). HPIV3 outbreaks typically happen in spring or early summer. Once infected with HPIV3, the virus replicates inside epithelial cells of the respiratory tract. If the infection is limited to only the nasal and throat passages the result is usually an upper respiratory tract infection, or cold. In healthy individuals, this is the most common outcome of HPIV3 infection. Occasionally, the infection spreads beyond these parts of the respiratory tract to the lower respiratory tract where more severe diseases can occur (10). If HPIV3 progresses to the lower respiratory tract, particularly common in young children and elderly individuals, severe lower respiratory illnesses such as bronchiolitis, pneumonia, and croup result. For example, in young children HPIV3 is the second leading cause of bronchiolitis and pneumonia behind respiratory syncytial virus (RSV) (10-13). There are approximately 500,000 to 800,000 hospitalizations in the United States due to lower respiratory tract infections in individuals under the age of eighteen, with HPIV3 accounting for 12% of these cases (9,14-16). In developed countries, such as the United States, mortality due to HPIV3 is highly unusual, and is almost exclusively limited to infants and immunocompromised and elderly individuals (11).

There is no vaccine or antiviral therapy available for HPIV3. Fortunately, most upper respiratory infections are self-limiting. However, for severe cases of croup, bronchiolitis, or pneumonia, treatments such as epinephrine or corticosteroids could be beneficial to help relieve symptoms and open up the airway passage (4,17-19). Overall, HPIV3 is a major public health and economic concern due to how common it is, and the number of doctor visits and hospitalizations it causes.

Structure

HPIV3 is negative sense RNA virus that is non-segmented, enveloped, pleomorphic with particles about 150-200 nm in diameter (4,9,20). The HPIV3 genome is about 15,000 nucleotides and encodes seven major proteins, nucleocapsid (N), phosphoprotein (P), C, matrix (M), fusion (F), hemagglutinin-neuraminidase (HN), and large (L); all proteins are structural except the C protein (Figure 1; 4,9,21).

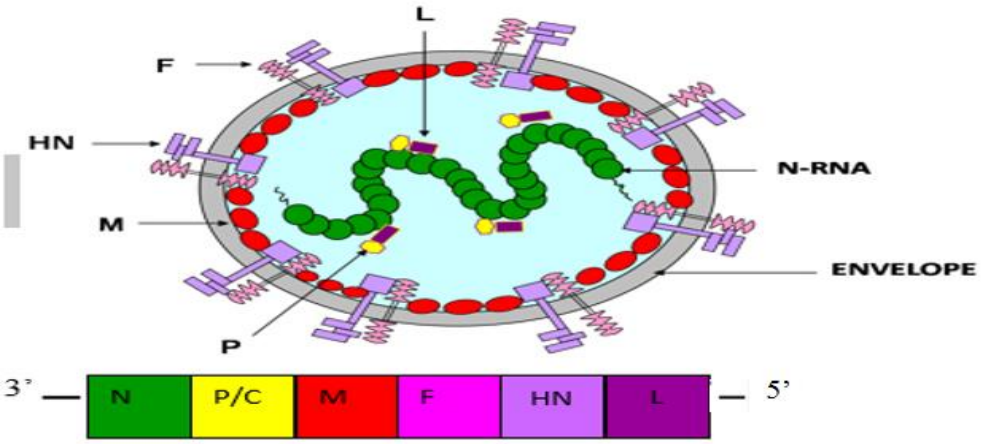

FIG 1 HPIV3 major proteins encoded by the genome. See text for more.

HPIV3 has an envelope that is acquired when the virus buds from a host cell plasma membrane. The hemagglutinin-neuraminidase (HN) and fusion (F) glycoproteins are transmembrane proteins in the viral envelope (9,18-20). The majority of these proteins extend outward from the envelope. The HN protein allows the virus to attach to the host cells by binding to sialic acid residues on proteins of the host cell membranes. The sialic acid binding activity of this protein is also responsible for the ability of HPIV3 particles to agglutinate red blood cells (hemagglutination). The neuraminidase activity of

HN cleaves sialic acid residues from host cell membrane proteins. (22-24). The F protein mediates fusion of the viral envelope and the host cell plasma membrane.

In the interior of the particle, the viral RNA is bound by the nucleocapsid (N) protein which forms a helical N-RNA structure. The large (L) polymerase and phosphoprotein (P) proteins bind to the N-RNA, forming the ribonucleoprotein complex (RNP) (4,9). The L and P proteins work together and act as the RNA-dependent RNA polymerase (RDRP) for viral transcription and replication (4,9).

The matrix (M) protein is membrane-associated on the interior of the viral envelope. This protein is the most common structural protein in the viruses of the *Mononegavirales* order (4,9,24). The M protein mediates virus particle assembly and release. During assembly, the M protein binds to other viral proteins to coordinate the assembly process. How the M protein is used to trigger budding of virus particles from cells is still not well understood.

The C protein of the paramyxoviruses is not a structural protein, but has been shown to have roles in inhibiting viral transcription, promoting virus budding, and counteracting host immune responses (21,25,26).

Life Cycle

Attachment is the first step in the life cycle and begins when HN binds to sialic acid residues on the host cell proteins present on a cell's plasma membrane. After this, the F protein mediates fusion of the viral envelope and the cell membrane. Once the virus envelope and cell membrane have fused, the RNP enters the host cell's cytoplasm (4,27,28). The P and L proteins make up the RDRP which is needed for transcription and

replication of the viral genome (3,4,9). The RDRP starts transcription on the 3' end of the genome and makes six viral mRNAs for N, P/C, M, F, HN, and L. After transcription, the host cell ribosomes translate the mRNAs into proteins. The negative sense, genomic RNA can then serve as a template for replication. After genome replication and further synthesis of viral proteins, assembly occurs. The first step in this process is the formation of the helical N-RNA structure, to which the P and L proteins bind to form the RNP complex. Next, viral components assemble at the cytoplasmic side of the cell membrane. It is thought that the M proteins guides the assembly process by binding to other viral proteins to coordinate assembly. M associates with the RNP complex (by binding to N) and binds to the cytoplasmic tails of the HN and F proteins (3,4,20,29). Once all viral components are present at the plasma membrane, budding takes place. This process allows viruses to exit the host cell. Prior to and during the assembly/release process, the neuraminidase activity cleaves the sialic residues off all cell surface proteins including HN and F proteins. This ensures efficient release and spread of newly formed virus particles by preventing virion-virion binding and the reattachment of released virions to the previously infected host cell (4,25,30,31).

Matrix Protein of the *Mononegavirales*

The M protein assists in assembly and release of virus particles (32). It is well understood how the M protein assembles virions, but less is known about the role of M proteins in triggering budding from the cell. It is known that matrix proteins have the ability to trigger budding without any other viral proteins present. When expressed individually in cells, M proteins of many paramyxoviruses including HPIV3, RSV, SeV, HPIV1, Nipah virus (NiV), and MeV can produce virus-like particles (VLPs; 3,4,9,33-

45). These VLPs are composed of a lipid membrane surrounding the M protein. However, some paramyxoviruses such as PIV5 and MuV require coexpression of the matrix protein with other viral proteins (N and F or HN) to form VLPs (46,47). In any case though, the M protein is essential for budding from the host cell.

Another known activity of some *Paramyxoviridae* M proteins is nuclear transit. For NiV, Hendra (HeV) SeV and MuV viruses it has been found that nuclear transit is required for the M protein-triggered budding (48,49). Nuclear transit of the M protein is important for budding, yet the reason why is unknown. However, it is thought that the M protein could be modified in a way that is essential for budding. Additionally, M could enter the nucleus to interfere with host functions such as transcription, while in the nucleus.

Late Domains

As previously stated, the mechanism through which release of VLPs/virus particles occurs is still unclear. Late domains, which are short, defined amino acid sequences, are needed on some M proteins to facilitate budding from the host cell (50). There is evidence that late domains bind cellular proteins involved in vesicle formation and redirects these proteins to the plasma membrane where they trigger virus budding. Late domains have been found in some members of the *Mononegavirales*, mostly in the *Filoviridae* and *Rhabdoviridae* (51).

In cells, plasma membrane proteins that play a key role in maintaining homeostasis are either degraded or recycled. Proteins that are targeted for degradation are mono-ubiquitinated after endocytosis. This allows these proteins to be recognized by a

series of cellular protein complexes, collectively termed the endosomal sorting complex required for transport (ESCRT) system. The ESCRT system, by facilitating vesicle budding into endosomes to form multivesicular bodies (MVBs), mediates sorting of proteins that were on the cell membrane to the lysosome for degradation or back to the cell membrane for reuse (52-54).

Enveloped viruses containing proteins with late domains are able to bind cellular ESCRT proteins and hijack the ESCRT machinery and can take it to the plasma membrane to initiate virus budding, thus facilitating virus release (Figure 2). Identification of late domains in the *Paramyxoviridae* has not been as straight forward as in other families. SeV is the only paramyxovirus shown to have an interaction between M and an ESCRT protein (Alix). This interaction was shown to be late domain-dependent and needed for virus budding (55-58).

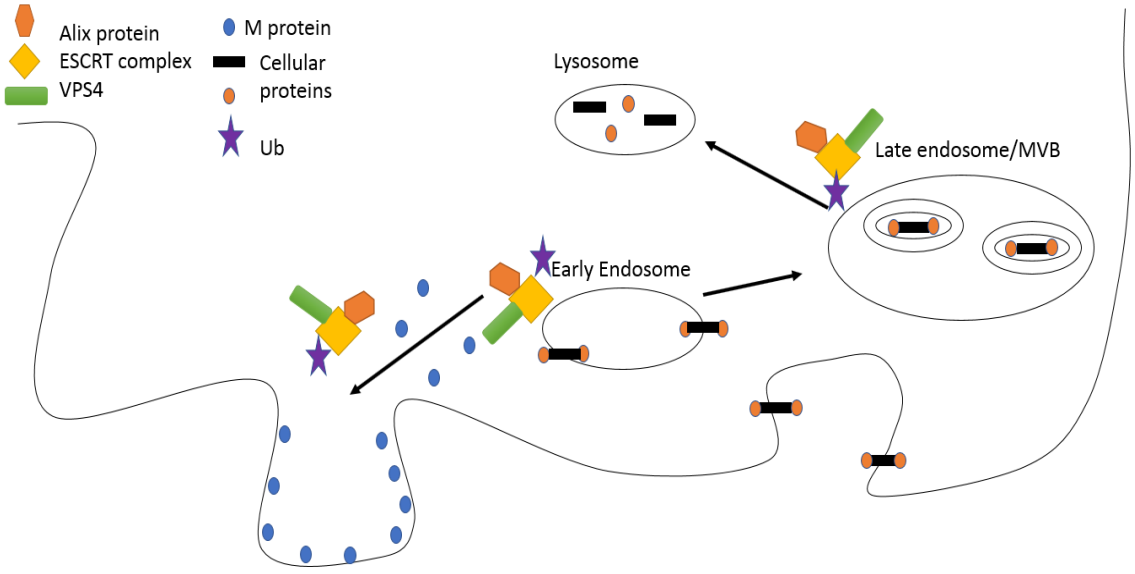

FIG 2 ESCRT associated viral budding. This figure demonstrates the ESCRT pathway being used by some mononegavirus M proteins to facilitate budding.

Nuclear Trafficking and NLS and NES Signals/Domains

It had been previously thought that paramyxoviruses replicate entirely in the cytosol. However, it is clear that nuclear trafficking of M is important in some paramyxovirus life cycles. Recent data has shown that nuclear trafficking is a prerequisite for M protein to function in budding. The exact reasons for nuclear trafficking of M are not yet known.

The mechanics of M protein nuclear localization and export are understood for paramyxoviruses. Nuclear localization (NLS) and nuclear export signals (NES) found within the M proteins are thought to regulate transient nuclear localization (48). An NLS is a lysine/arginine rich sequence that allows a protein to interact with the nuclear cargo receptor (NCR), also called Importin, which mediates importation of proteins into the nucleus. The NES is a leucine rich sequence that interacts with the complex of the NCR and Ran-GTP, also called Exportin, which promotes export of the protein from the nucleus. By sequence alignment, the M protein NLS and NES domains appear to be conserved throughout the *Paramyxovirinae* subfamily. Both NLS and NES sequences are functionally conserved in NiV, HeV, SeV, and MuV. Thus, via this alignment, putative NLS and NES sequences in the HPIV3 M protein have been identified (Figure 3).

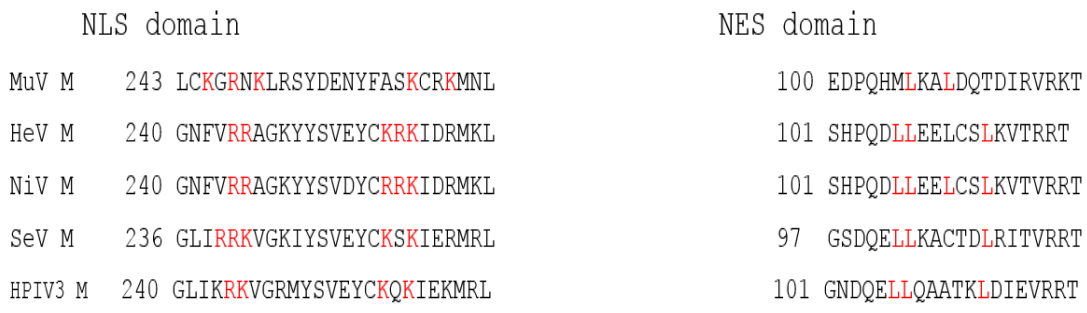

FIG 3 Conserved NLS and NES signals in the *Paramyxovirinae* subfamily. The amino acids in red are predicted to be critical amino acids for nuclear transit (modified from 48, 59-62).

Nipah virus was the first paramyxovirus investigated for M protein nuclear trafficking. NiV was shown to have NLS and NES signals that regulate nuclear-cytoplasmic trafficking. Mutations of conserved residues in the NLS led to nuclear exclusion, while mutations in conserved residues in the NES led to increased nuclear accumulation. Furthermore, it was demonstrated that nuclear export was also regulated by ubiquitination, which takes place in the nucleus. Ubiquitination occurs on a lysine residue (K258) located within the NLS of the M protein of NiV. A K258R mutant, which conserves a functional NLS and retains nuclear localization function, was not ubiquitinated and was defective in nuclear export, indicating that ubiquitination was important for nuclear export. All NLS and NES mutants have reduced VLP formation ability. Also, it was found that proteasome inhibition results in nuclear retention of the M protein. Proteasome inhibition results in polyubiquitinated proteins not being degraded. Thus, Ub was not recycled and free Ub is depleted, resulting in decreased ubiquitination of proteins. Under this condition, the NiV M protein was retained in the nucleus, again pointing to the importance of ubiquitination in the nuclear export of the M protein.

In summary, nuclear cytoplasmic trafficking was a prerequisite for NiV M budding. Specifically, the NLS was needed for the NiV M protein to go into the nucleus, where it is ubiquitinated within the NLS domain. Ubiquitination appears to be needed for nuclear export. It was proposed that the ubiquitinated M protein then interacts with proteins of the ESCRT pathway to facilitate budding (48,49). However, no known interaction between any ESCRT protein and the NiV M protein has been demonstrated.

Nuclear transit and ubiquitination have also been observed in other paramyxoviruses. Nuclear transit of the M proteins of NiV, HeV, SeV, and MuV was controlled by an NLS. When the lysine (K258 in NiV) in the NLS was mutated to an alanine nuclear exclusion was seen. When this lysine was changed to an arginine a decrease in ubiquitination and an increase of nuclear retention was seen. Increased nuclear localization of these M proteins was also seen when ubiquitin was depleted. Additionally, in HeV, SeV, and MuV mutation of the leucines in the NES cause significant nuclear retention compared to their respective wild-type proteins (48).

To summarize, nuclear trafficking of the M protein was regulated as follows. After the M protein enters the nucleus via a NLS, it is ubiquitinated on a lysine present within the NLS. This is thought to prevent nuclear re-entry because after ubiquitination, importin (the cellular protein that recognizes the NLS) can no longer bind. Thus, ubiquitination, in addition to the NES, was also needed for nuclear exclusion (48,49). It is thought that the ubiquitination of M proteins allows recognition of ESCRT complexes which help mediate budding of many enveloped viruses, such as HIV and Ebola (48,63-65). However, with the paramyxoviruses there is minimal evidence showing that M proteins can bind to ESCRT proteins, let alone in ubiquitin-dependent manner. Overall

though, ubiquitination of M proteins is critical for M protein function and is needed for nuclear exit.

HPIV3 NLS and NES

Putative NLS and NES motifs in the HPIV3 M sequence have been identified (Figure 3). Alignment of the HPIV3 M sequence with other paramyxoviruses, shows that NLS and NES domains could be located at 240-GLIKRKVGRMYSVEYCKQKIEKMRL-260 and 101-GNDQELLQAATKLDIEVRRT-120 respectively. Lysines that are needed for NLS function, and leucines that have been shown needed for NES function in SeV are conserved in HPIV3 (Figure 3; 48,49,59-62). Because of this it is possible that the M protein of HPIV3 also undergoes nuclear trafficking.

In the past the Hoffman lab has investigated M nuclear localization with immunofluorescent (IF) based analysis of cells transfected to express HPIV3 M_F, a carboxy-terminal flag tagged version of M. The M protein was primarily located in the cytoplasm, but some M_F was also detected in the nuclei of cells (Hoffman lab unpublished data). However, past results in the Hoffman lab have shown issues with tagged versions of HPIV3 M. HPIV3 M proteins with HA or Flag tags at the amino- or carboxy-termini were shown to bud as VLPs about two-fold less efficiently than wild-type M (42). Additionally, recovery of virus from an infectious clone encoding a carboxy-Flag tag on M was unsuccessful, indicating the Flag sequence had a severe, negative effect on the life cycle of the virus (personal communication, M Hoffman). Because of this, we wanted to use the wild-type M protein for further localization studies, which necessitated development of a specific antibody for the M protein.

RESEARCH OBJECTIVES

Nothing is known regarding nuclear trafficking and the putative NLS and NES domains of the HPIV3 M protein. To better understand how the M protein facilitates budding, my research will examine nuclear trafficking of the HPIV3 M protein and if the putative NLS and NES signals are involved in this process. After establishing an IF-based localization assay for the M protein, I will create mutants in the NLS and NES domains to see their impact on M protein localization and release of VLPs.

Specific Objectives

1. Develop an M protein localization assay.
2. Examine whether putative NLS and NES domains affect M protein localization and release of virus-like particles.

MATERIALS AND METHODS

Cells

293T (human embryonic epithelial kidney cells) cells were cultured in Dulbecco's modified Eagle's medium (DMEM) with 10% fetal bovine serum (FBS), and grown at 37°C with 5% CO_2. HeLa cells were cultured in DMEM with 5% FBS and grown at 37° C with 5% CO_2.

Plasmids

The pCAGGS M plasmid was previously constructed by inserting the HPIV3 M-encoding sequence into the pCAGGS eukaryotic expression vector (42). The NLS mutants K258A, K258R, and the NES mutant L106/107A were created through PCR-based site-directed mutagenesis of the pCAGGS-M plasmid.

Primary Antibody Development

An anti-M polyclonal antibody was developed to use in M protein localization assays. The Hoffman lab worked with Li International to develop the antibody. Based on hydrophilicity, Li International suggested several regions of the M protein as possible peptides to be used for immunization. Further analysis was done by aligning and overlaying the HPIV3 M protein sequences into the sequence/crystal structure of Newcastle virus M protein (no crystal structure of the HPIV3 M protein is available) to further confirm that the peptide would be on the surface of the protein. It was decided to

use the 50 amino acid sequence 214-263:

VQTDSKGIVQILDEKGEKSLNFMVHLGLIKRKVGRMYSVEYCKQKIEKMR to develop the primary antibody. Li International produced the peptide and immunized two rabbits.

Characterization of the Primary Antibody

Transfections were performed with 30-40% confluent 293T cells in 6 well plates. The M plasmid, 0.5 µg, was added to 120 µl Opti-MEM™ (Gibco™ by Thermo Fisher Scientific) and 3 µl X-tremeGENE™ 9 DNA transfection reagent (Roche) at room temperature, allowed to sit for 30 min and then added to the cells. After 48 hrs post transfection cells were lysed with 400 µl of 1X cell lysis buffer (25 mM tris-phosphate, 2 mM dithiothreitol (DTT), 2 mM ethylenediaminetetraacetic acid (EDTA), 10% glycerol, 1% Triton-X100, pH 7.6), and centrifuged for 10 min at 2,567 RCF. Then the supernatant was collected and used to run a western blot. 10 µl of the supernatant was then added to 10 µl of 4X SDS buffer and heated to 95 ºC for 5 min prior to electrophoresis by SDS-PAGE on 0.75 mm 12% acrylamide gels. Proteins were transferred from the gel to Immobilon®-P polyvinylidene difluoride (PVDF) (Milipore®) membranes with a semi-wet transfer system at 3 volts and 0.19 amps for 45 min. After the transfer, the membrane was blocked overnight at 4°C with 5% milk in Tris-buffered saline with Tween® 20 (TBST) (150 mM NaCl, 50 mM Tris-Cl, 0.05% Tween® 20, pH 7.5). After blocking, membranes were incubated with the polyclonal rabbit anti-M protein antibody (Li International) in TBST (1/100 and 1/200 dilutions) for 1 hr. Then the membranes were washed three times with 5% milk/TBST and then three times with TBST. Next the membranes were incubated with a secondary antibody, donkey anti-rabbit HRP antibody

(SA1-100, Thermo Scientific) in TBST (1/2000 dilution) for 1 hr. Then the membranes were washed three times with 5% milk/TBST and then with TBST three times. Following the secondary antibody, all membranes were exposed to SuperSignal® West Pico Chemiluminescent Substrate (Thermo Scientific), and visualized with a ChemiDoc™ Touch (Bio-Rad®) imaging system. All images were analyzed with Image Lab™ (Bio-Rad®).

Immunofluorescent Microscopy

Sub-confluent (40%) 293T cells on glass coverslips were transfected with pCAGGS-M, or NLS/NES mutants thereof. At varying time points post-transfection, cells were fixed with 4% formaldehyde for 10 min, permeabilized with 0.5% Triton X-100 (Sigma) in PBS twice for 2 min, and blocked with 5% milk in TBST for 30 min. The coverslips were incubated with the rabbit anti-M protein (1/100 dilution in TBST) for 1 hr, washed three times with TBST, and followed by a 1 hr incubation with a goat anti-rabbit IgG antibody conjugated with Dylight 594 (1/200 dilution in TBST) (Abcam96885 courtesy of Dr. Sanderfoot). Cells were washed twice with TBST, and incubated with 300 nM of DAPI (Thermo Fisher) in PBS for 5 min, then washed three times with PBS. The coverslips were then mounted on microscope slides with one drop of Fluoromount-G® (Southern Biotech) and sealed. A Nikon Eclipse 80i microscope and a Nikon CS1 Laser Scanning confocal fluorescence microscope were used for microscopic analysis, and images were analyzed with ImageJ (National Institutes of Health). To quantify the amount of M protein present in the nucleus the integrated density in the nucleus and the integrated density of the total M protein present was determined. The integrated density of the M protein in the nucleus was divided by the integrated density of the M protein

present throughout the whole cell to find the percent of the M protein present in the nucleus.

To determine the localization of the M protein in HPIV3-infected cells, HeLa cells were infected with HPIV3 at an MOI of either 0.1, 1, or 10. The IF procedure was identical to the IF procedure listed above, cells were fixed at 24 hr, blocked, incubated with antibodies, counter stained with DAPI and viewed with fluorescence and confocal microscopy.

Virus-Like Particle Budding Assays

Transfections were performed with 30-40% confluent 293T cells in 6-well plates. Plasmids were added to 120 µl Opti-MEM™ (Gibco™ by Thermo Fisher Scientific) and 3 µl X-tremeGENE™ 9 DNA transfection reagent (Roche) at room temperature, and let sit for 30 min. The amount of each plasmid used for transfections were as followed: 1.2 µg of M, 0.6 µg K258A, 1.0 µg K258R and 1.2 µg L106/107A.

To collect the HPIV3 M protein released into the media as VLP's, the media was collected 48 hr post transfection, and centrifuged for 10 min at 9495 RCF. The supernatant was then layered on top of 3.2 mL of a 20% sucrose solution in phosphate-buffered saline (PBS) (8 mM Na_2HPO_4, 137 mM NaCl, 2 mM KH_2PO_4, 2.7 mM KCl) and subjected to ultra-centrifugation at 121,570 RCF to pellet VLP's. Pellets were resuspended in 20 µl 6X SDS running buffer. Cell lysate samples were taken by adding 400 µl of 1x cell lysis buffer to the cells, and allowing 5 min for lysis. The collected lysate was then centrifuged at 9495 RCF for 10 min. The supernatant was collected and 8 µl of sample was added to 3 µl of 6X SDS buffer. Media and lysate samples were heated

at 95°C for 5 min, then subjected to SDS-PAGE on a 0.75 mm 12% acrylamide gel for western blot analysis as previously described. However, to detect the HPIV3 M protein, membranes were incubated with the polyclonal rabbit anti-RNP antibody (Courtesy of the Amiya Banerjee lab at Cleveland Clinic) in TBST (1/2000 dilution) for 1 hr instead of the anti-M antibody used during the primary antibody development protocol listed above.

RESULTS

Objective 1: Develop an M Protein Localization Assay.

To develop a means to assess M protein localization in cells, an IF-based localization assay was developed. In an IF-based protein localization assay, antibodies against the target protein are critical. To develop the assay, we had an anti-M polyclonal antibody made by Li Technologies. The Hoffman lab worked with the company to design a 50 amino acid segment of matrix protein, aa 214-263 (VQTDSKGIVQILDEKGEKSLNFMVHLGLIKRKVGRMYSVEYCKQKIEKMR) that was used as an antigen and injected into rabbits to generate an antibody. After we received the antibody, it was characterized in a western blot to ensure binding to the M protein of HPIV3 (Figure 4). The rabbit anti-M antibody was able to bind the M protein (Lane 1, Figure 4). However, there also was evidence that the antibody might not be completely specific for the M protein as the antibody bound cellular proteins in mock transfected cells (Lane 2, Figure 4).

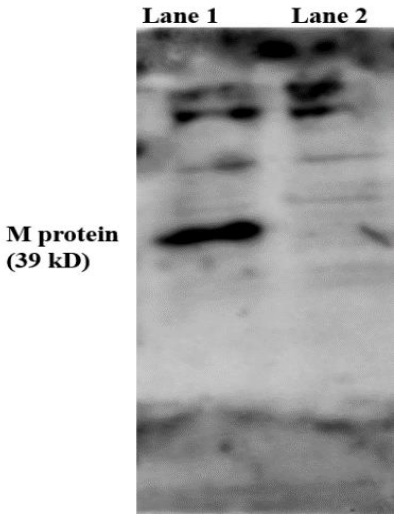

FIG 4 Testing the anti-M antisera for detection of HPIV3 M protein. Forty-eight hr post-transfection, cellular lysates were collected. Proteins were separated via SDS-PAGE and the M protein was detected through a western blot. A cytoplasmic extract from cells transfected to express the M protein was run in Lane 1, while proteins from a mock transfection were run in Lane 2.

The antibody was then tested with an IF-based localization assay to confirm the antibody was able to visualize the M protein. 293T cells on coverslips were transfected with a plasmid encoding the HPIV3 M protein. Variables tested during the development of the assay included time of staining post-transfection, and primary antibody dilutions. The cells were also counter-stained with DAPI, which allows visualization of the nuclei.

After repeating the experiment four times it was clear that all conditions tested yielded similar results (Figure 5). A 1/100 dilution of the primary antibody and 24 hr post transfection time point was used for all further experiments to do experiments more rapidly and to potentially decrease non-specific staining of the antibody.

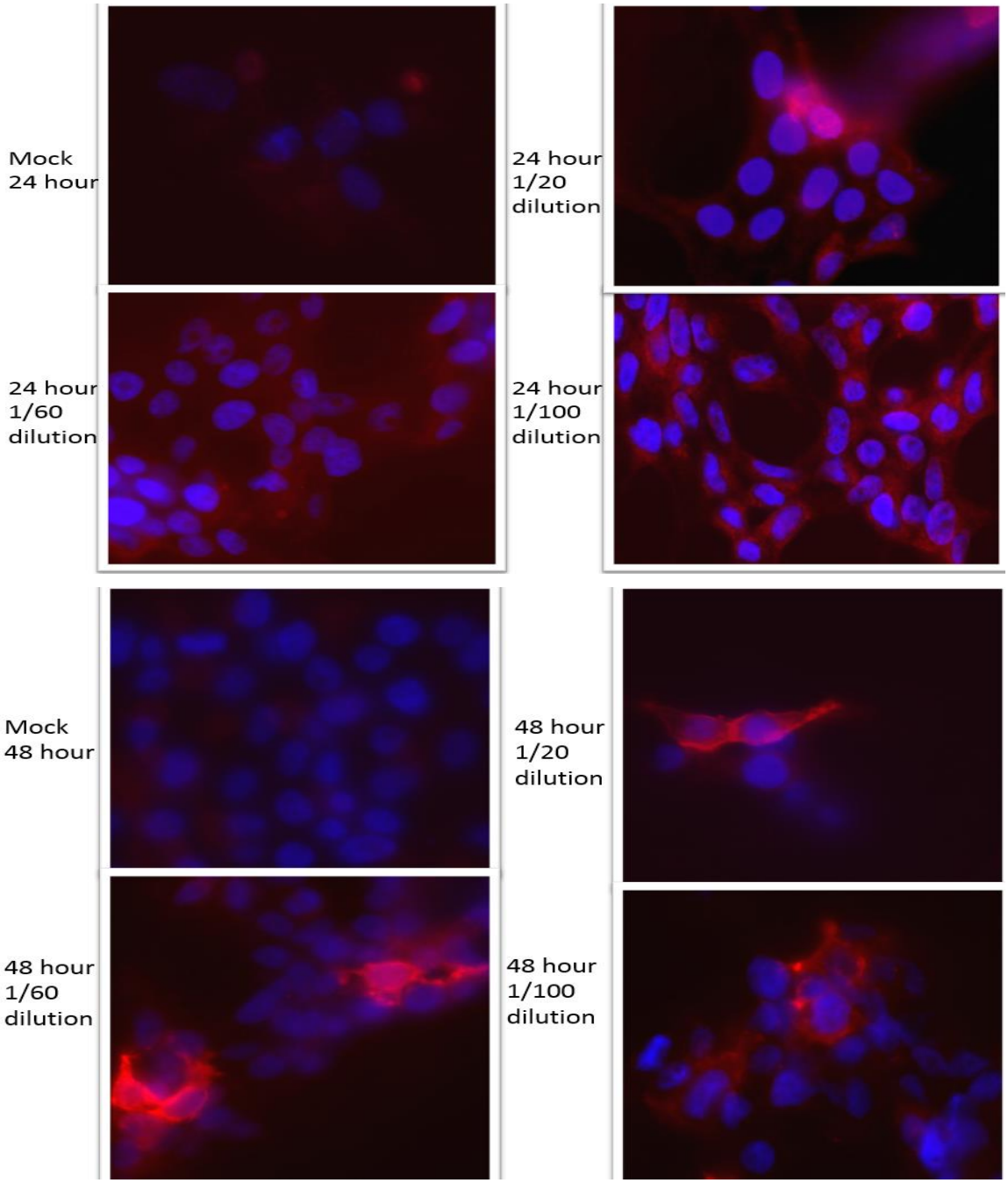

FIG 5 HPIV3 M protein localization assay development in 293T cells. 0.5 µg of M was transfected into 293T cells on coverslips. At 24 and 48 hr post-transfection, cells were fixed with 4% formaldehyde, permeabilized with 0.5% Triton X 100, and blocked with 5% TBST milk. Then the samples were incubated with rabbit anti-M primary antibody, either 1/20, 1/60, 1/100 dilution, followed by a secondary antibody conjugated with Dylight 594. DAPI was used for visualization of the nuclei. Samples were imaged at 600x with epifluorescence microscopy.

After the assay was developed the transfected M protein was examined via confocal microscopy to determine the degree of M protein nuclear localization. The integrated density of the M protein in the nucleus and the entire cell was determined for approximately 30 different cells to determine the portion of M in the nucleus. At 24 hr post-transfection 65.3% $\pm$15.1 of the M protein was present in the nucleus (Figure 6).

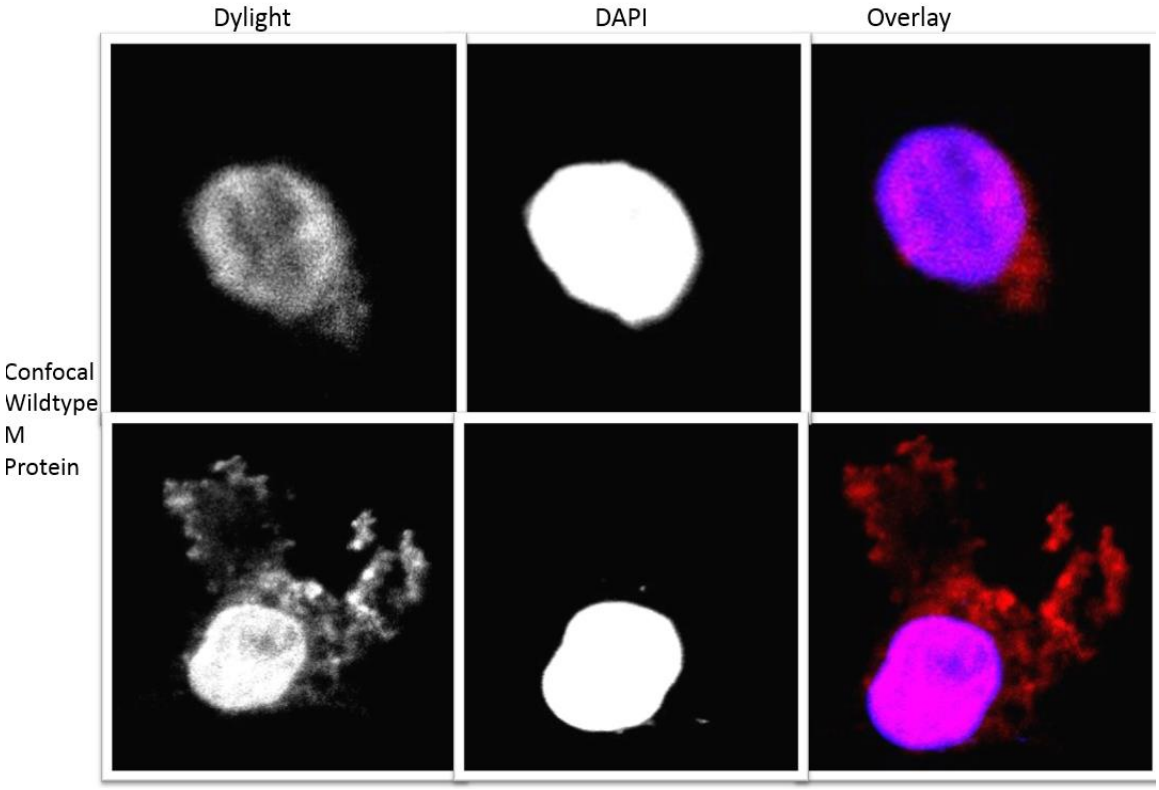

FIG 6 HPIV3 M protein nuclear trafficking in 293T cells during a transfection. 0.5 µg of M protein was transfected into 293T cells on coverslips. At 24 post-transfection, cells were fixed with 4% formaldehyde, permeabilized with 0.5% Triton X 100, and blocked with 5% TBST milk. Then the samples were incubated with rabbit anti-M primary antibody, followed by a secondary antibody conjugated with Dylight 594. DAPI was also added to visualize the nuclei. Cells were imaged at 600x with confocal microscopy. Samples were quantified with ImageJ.

After the assay was developed with transfected cells, it was applied to HPIV3-infected HeLa cells to confirm the assay was functional and to see if the M protein in the

context of a virus infection follows the same pattern as with transfection-expressed M protein. HeLa cells were infected at MOIs of 0.1, 1, and 10 and were analyzed by IF at 24 hr post infection. In the mock samples little to no red background was seen, which confirms that the primary antibody is fairly specific for the viral M protein. The infection with an MOI of 1 was found to be most useful, as some cells were infected, some not infected, and syncytia (cells that fused together as a result of HPIV3 infection) were present. The MOI of 10 was too much virus when assayed at 24 hr post-infection since many cells had detached from the coverslips and those remaining showed extensive cytopathic effects (Figure 7).

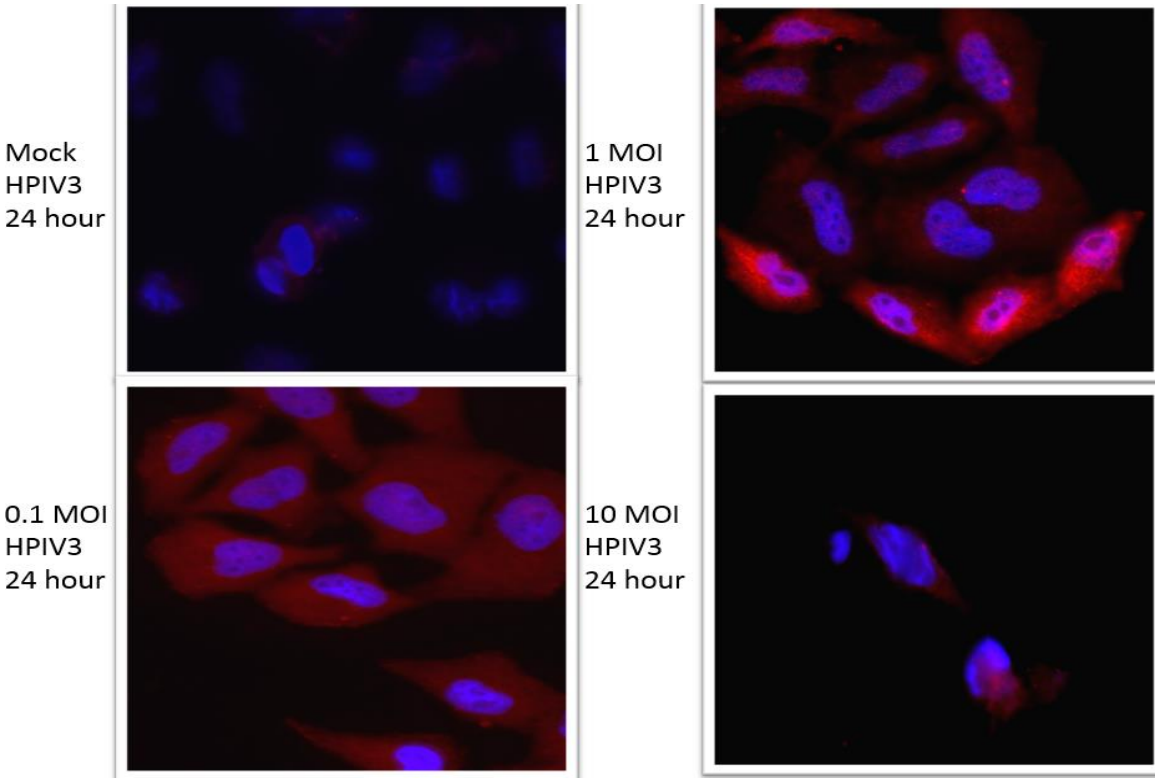

FIG 7 Detection of M protein in HPIV3-infected cells. HPIV3 was infected at a MOI of 0.1, 1, and 10 into HeLa cells on coverslips. At 24 post-infection, cells were fixed with 4% formaldehyde, permeabilized with 0.5% Triton X 100, and blocked with 5% TBST milk. Samples were then incubated with rabbit anti-M primary antibody, followed by a secondary antibody conjugated with Dylight 594. Cells were stained with DAPI to visualize the nuclei. Cells were then imaged at 600x with epifluroescent microscopy.

The samples were then viewed with confocal microscopy to quantify nuclear localization. With an MOI of 0.1, 47.9% $\pm$ 2.45 of the M protein was found to be in the nucleus at 24 hr and with an MOI of 1, 53.4% $\pm$ 13.7 of the M protein was found to be in the nucleus (Figure 8). This shows that the M protein does truly localize to the nucleus.

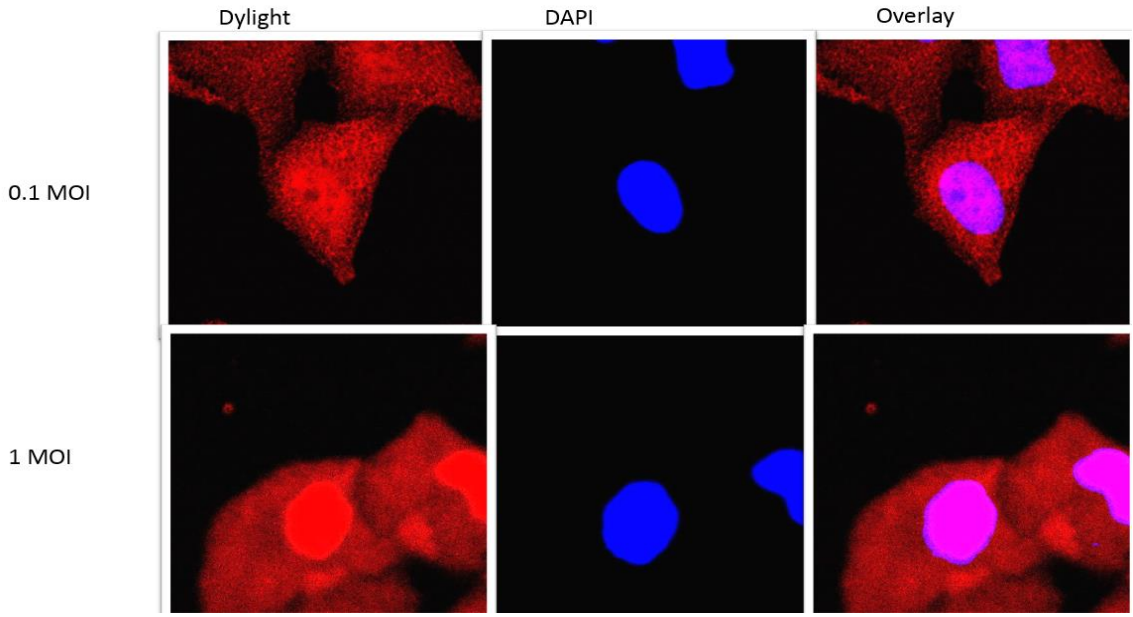

FIG 8 Quantification of M protein in HPIV3 infected cells. HPIV3 was infected at a MOI of 0.1 and 1 into HeLa cells on coverslips. At 24 post-infection, cells were fixed with 4% formaldehyde, permeabilized with 0.5% Triton X 100, and blocked with 5% TBST milk. Then samples were incubated with rabbit anti-M primary antibody, followed by a secondary antibody conjugated with Dylight 594. DAPI was used for visualization of the nuclei. Cells were imaged at 600x with confocal microscopy. Images were quantified with ImageJ.

Objective 2: Examine Whether Putative NLS and NES Domains Affect M Protein Localization and Release of Virus-Like Particles.

Since the IF assay shows M localization to the nucleus, the functions of the putative NLS and NES signals were tested. Specifically, in the NLS, K258A and K258R mutants were made and in the NES two critical leucines (aa 106 and 107) were mutated simultaneously to alanines. The K258A mutant was constructed because a basic residue at aa258 should be critical for nuclear localization signal function, and previous studies using an analogous mutant with Nipah, Hendra, Mumps, and Sendai virus M proteins prevented the M protein from entering the nucleus (48, 49). The K258R mutant (which

maintains the basic amino acids of the NLS) was created because this mutation with NiV, HeV, SeV, MuV, and NDV still entered the nucleus, but then accumulated there (48, 49). This observation was correlated with the K258R mutant not being ubiquitinated at K258, which does occur with the wild-type M protein (48, 49). Similarly, in previous studies with NiV, HeV, and SeV viruses it was seen that changing the leucine residues at 106/107 in the NES to alanines caused the M protein to accumulate in the nucleus (48, 49). To confirm expression and detection of the mutant proteins, epifluorescence was used to observe each mutant and wild-type M protein. All proteins were detected via the immunofluorescence assay (Figure 9).

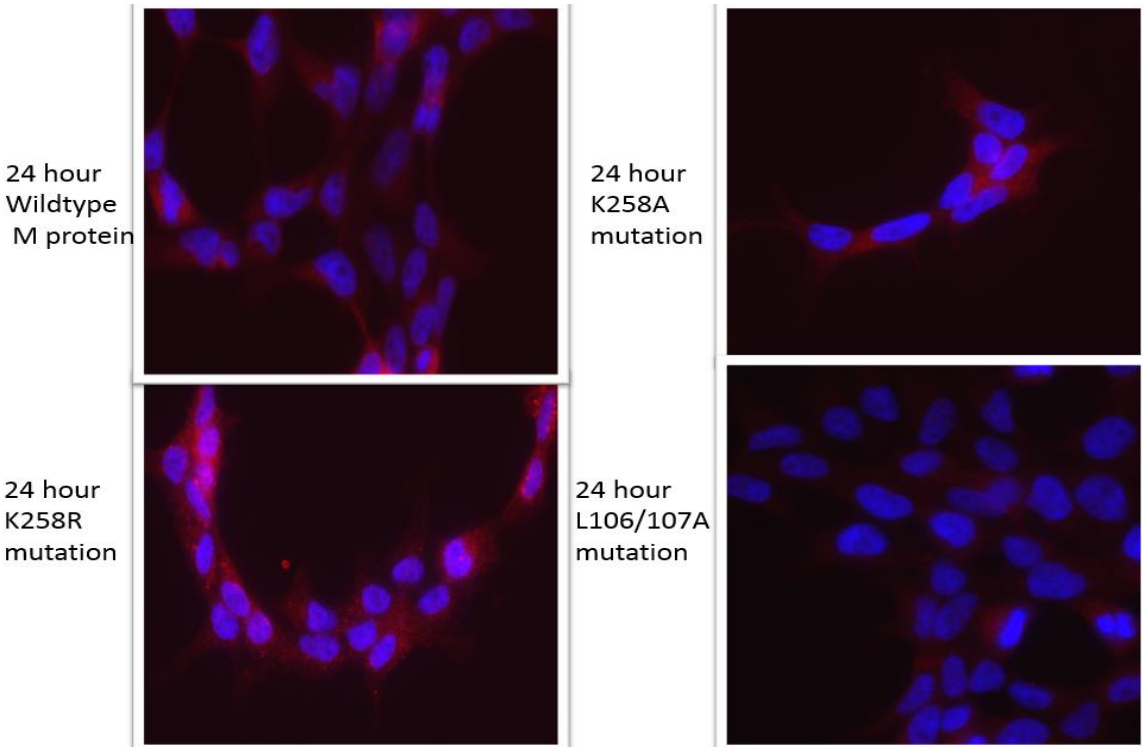

FIG 9 HPIV3 M protein and mutant analysis in 293T cells. 0.5 µg of M, K258A, K258R, and 106/107A were transfected into 293T cells on coverslips. At 24 hr post-transfection, cells were fixed with 4% formaldehyde, permeabilized with 0.5% Triton X 100, and blocked with 5% TBST milk. Samples were then incubated with rabbit anti-M primary antibody followed by a secondary antibody conjugated with Dylight 594. Cells were stained with DAPI to visualize the nuclei. Samples were imaged at 600x with epifluorescent microscopy.

Next the samples were viewed with confocal microscopy to more accurately quantify nuclear localization. When analyzing M protein mutants, statistically significant differences in nuclear localization were seen when compared to wild-type M: 38.0% $\pm$ 16.6 of the K258A mutant, 82.8% $\pm$ 9.8 of the K258R mutant and 80.0% $\pm$ 7.7 of the L106/107A mutant was found in the nucleus at 24 hr (Figure 10, 11). These results follow suit with the expected results from previous studies.

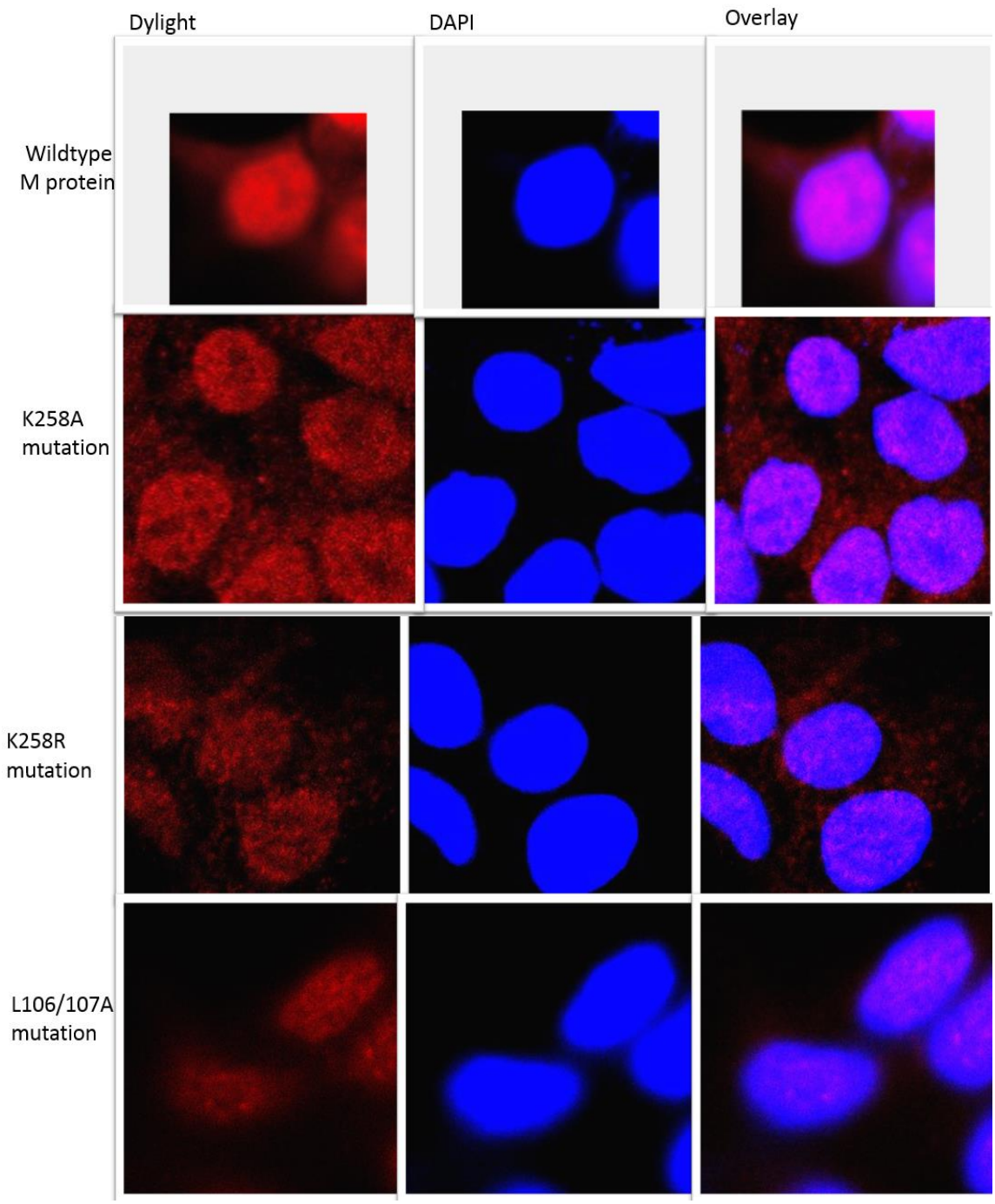

FIG 10 HPIV3 M protein and mutant analysis of nuclear trafficking in 293T cells. 0.5 µg of M, K258A, K258R, and 106/107A were transfected into 293T cells on coverslips. At 24 hr post-transfection, cells were fixed with 4% formaldehyde, permeabilized with 0.5% Triton X 100, and blocked with 5% TBST milk. Then samples were incubated with rabbit anti-M primary antibody followed by a secondary antibody conjugated with Dylight 594. Cells were stained with DAPI to visualize the nuclei. Samples were imaged at 600x with confocal microscopy. Quantification was completed with ImageJ.

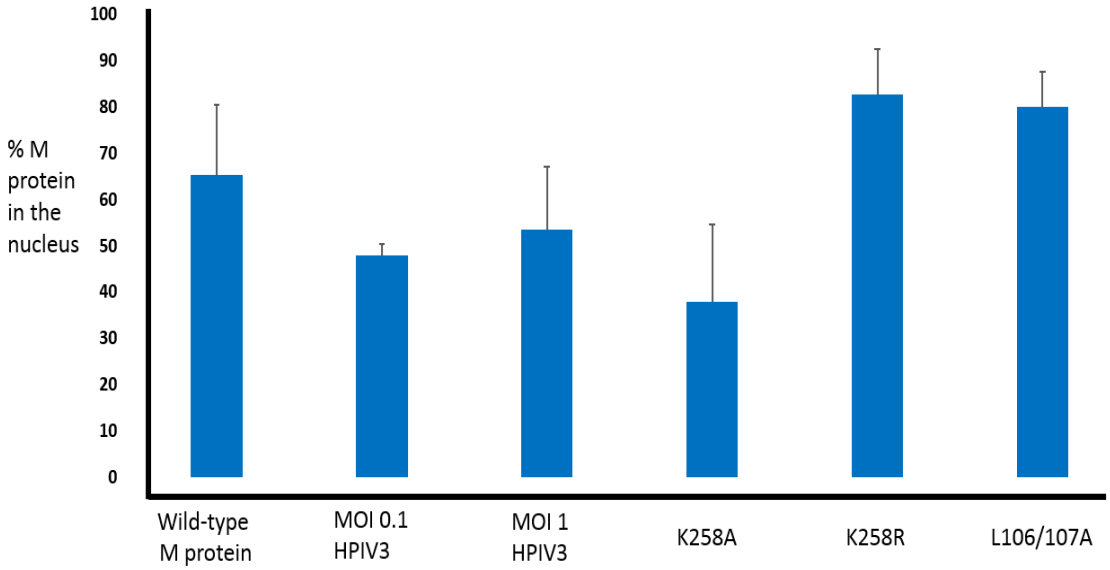

FIG 11 Quantification of M protein nuclear localization. Overall, all immunofluorescence data are represented in the graph. The means were calculated by finding the integrated density of M protein, the SD was calculated through a standard deviation formula, and P values were found through a standard t-test equation in excel. P values for the M mutants were as follows: K258A = 2.43×10^{-7}, K258R = 2.91×10^{-8}, and L106/107A = 3.38×10^{-6}.

The VLP formation ability of the mutants was also determined. 293T cells in 6-well plates were transfected with the pCAGGS clones encoding wild-type and NES and NLS-mutated M proteins. After 48 hr post transfection the media and lysates were collected. The VLP's were pelleted with ultracentrifugation of the media and the lysates samples were clarified by low speed centrifugation to remove cell debris prior to analysis by western blot. The M protein, K258A, and K258R were detected in the cell lysate samples (Figure 11 Lane 2, 3, and 4). However, after trying many different plasmid amounts of L106/107A in the transfection this mutant was not able to be detected (Figure 11 Lane 5). The wild-type M protein was able to bud from the cell (Figure 11 Lane 7). The K258A and K258R mutants showed greatly decreased budding at 5.6 and 6.2

percent, respectively, the release efficiency of wild-type M (Figure 11 Lane 8 and 9). Because the L106/107A mutant was not detected, its release efficiency could not be determined (Figure 11 Lane 10).

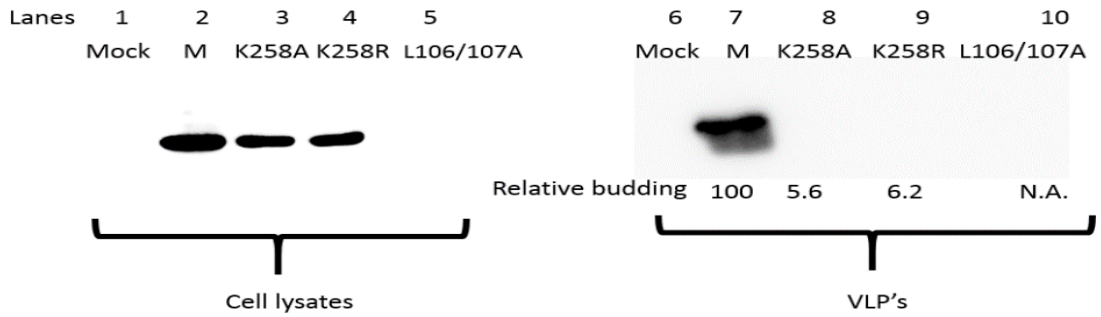

FIG 12 VLP release of HPIV3 M protein mutants. 293T cells in 6 well plates were transfected with 1.2 µg of M, 0.6 µg of K258A, 1.0 µg of K258R, and 1.2 µg of L106/107A. At 48 hr post-transfection media and lysate samples were collected. The VLP's were pelleted by ultracentrifugation at 121,5700 RCF and the lysates samples were centrifuged at 9495 RFC and the supernatant was collected. All samples were analyzed by western blot, visualized with a chemidoc imager, and analyzed with ImageJ.

DISCUSSION

With some paramyxoviruses, M protein nuclear transit is controlled by the NLS and NES domains. When these domains are disrupted nuclear transit is altered and budding fails to occur (48, 49). Thus, I investigated whether the M protein of HPIV3 also transits through the nucleus in an NLS/NES domain-dependent manner, and whether mutants defective in nuclear transit also show budding defects.

M protein localization was studied with indirect IF assays. The wild-type M protein was present in the nucleus as reported in other paramyxoviruses (48, 49). Specifically, approximately 50% of the transfection and infection-derived HPIV3 M protein was found in the nucleus 24 hr post-transfection (Figure 6, 8). Wang *et al.* likewise found 50% of 3X-Flag-tagged NiV M protein in the nucleus. They also looked at NiV M protein during an infection and saw M protein was distributed both in the nucleus and cytoplasm of infected cells, though they did not quantify the amount of M protein in the nucleus. Similarly, Pentecost *et al.* saw nuclear localization with SeV, NiV, HeV, MuV, MeV, and NDV. Specifically, Pentecost *et al.* saw approximately 30% nuclear localization with a 3X-Flag-tagged version of the SeV M protein. This contrast to my data could be due to the 3X-Flag-tag present on this virus, interrupting normal function of the M protein. Additionally, the difference could be due to the amount of plasmid used, or condition of cells used for the transfection (which impacts the level of protein expression). Pentecost *et al.* also viewed SeV localization during a live viral

infection. From their figures the amount of M protein located in the nucleus appears similar to my HPIV3 infection data, however, the exact amount located in the nucleus was not reported.

Since the M protein did localize to the nucleus the putative NLS and NES domains of M were investigated to determine if they could control nuclear transit and budding. K258 is a highly conserved lysine residue in the NLS and is believed to serve dual functions. The lysine is important for nuclear import; and serves as a ubiquitination site that appears to be important for nuclear export (48, 49). The K258A mutation, which reduces the positive charge of the NLS, was found to limit nuclear import in HPIV3 M protein transfection studies. Specifically, only 38% of the M protein was located in the nucleus (wild-type 65.3%) (Figure 10). Wang *et al.* showed that the mutation K258A in NiV 3X-Flag tagged protein also limited nuclear import, specifically they saw 38.5% in the nucleus (wild-type 50%) (49). In addition, Pentecost *et al.* also saw nuclear exclusion when mutating the lysine to an alanine in 3X-Flag-tagged SeV, NiV, HeV, and MuV, though they did not quantify the nuclear localization (48).

The mutation K258R, which maintains the positive charge in the NLS but ablates the ability of this position to be ubiquitinated, was also investigated in HPIV3. This mutation caused increased accumulation of M in the nucleus (82.8%) presumably due to decreased nuclear export or increased import (Figure 10). Wang *et al.* also mutated K258R in NiV and saw nuclear retention, specifically they found 62.5% of the M protein to be in the nucleus (49). Similarly, Pentecost *et al.* saw nuclear retention with SeV, NiV, HeV, MuV, and NDV when mutating this lysine in the NLS to an arginine. Specifically, 75-100% of the Flag tagged M protein was found in the nucleus with SeV, the virus most

closely related to HPIV3. As discussed in the introduction, ubiquitination occurs at lysine residues but not arginine residues thus in the nucleus K258R mutants are not ubiquitinated. It is also possible that ubiquitination of K258 is needed to change the conformation of the M protein to expose the NES to exportin, and thus without this change, the M protein is not able to leave the nucleus (49).

It is known with some paramyxoviruses that nuclear transit is needed for budding (48, 49). There are two main hypotheses for why the M protein travels through the nucleus. It is thought that the M protein may enter the nucleus to be modified to allow it to function in budding, and/or the M protein enters the nucleus to interfere with host functions. It is possible that ubiquitination of the M protein in the nucleus promotes recognition by ESCRT complexes, which are known to help mediate budding of some enveloped viruses. It is known that PIV-5, SeV and MuV M proteins can bind to ESCRT components and thus facilitate budding (48). The M protein of one paramyxovirus, RSV, enters the nucleus and appears to antagonize host functions by inhibiting host gene expression and inducing cell cycle arrest (48). Although, it is not exactly known why paramyxovirus M proteins travel through the nucleus, it has been deemed an important step of the viral life cycle because if you either impede nuclear import or export budding is inhibited (48, 49).

To further investigate the role of the NLS and NES on the budding process of HPIV3 M proteins VLP budding assays were conducted. Both wild-type M protein and the mutations K258A and K258R, were expressed. The K258A and K258R mutations abrogated budding ability. Similar to the Hoffman lab, Wang *et al.* observed that NiV K258A and K258R mutations also inhibited VLP budding (49). Specifically, they found

relative budding percentages for K258A and K258R less than 6% when compared to wild-type M VLP. Wang *et al.* wanted to find out if K258A could not bud due to conformational defect or lack of plasma membrane association, and thus ran membrane flotation assays. They confirmed that K258A had a lack of plasma membrane association and was not able to associate with the plasma membrane as well as wild-type M protein, which may explain why K258A cannot be packaged into VLP's. To understand if HPIV3 K258A M protein similarly cannot bud due to lack of membrane association a membrane flotation assay would be an essential next step. The increased nuclear retention of the K258R mutant could explain why budding is limited with this mutant. Additionally, because the HPIV3 M K258R mutant displayed nuclear retention, failed to bud from cells, and is predicted to not be ubiquitinated, a future experiment would be to investigate the ubiquitination status of this mutant.

The NES is a leucine rich sequence that controls nuclear export in some paramyxoviruses. An L106/107A double mutant in the HPIV3 M protein NLS was seen to have nuclear retention. Specifically, 80.0% of the M protein was found in the nucleus (Figure 10). Similarly, Pentecost *et al.* found that when mutating the two leucines to alanines in the NES nuclear retention was seen with the Flag-tagged M proteins of SeV, NiV, HeV, and MuV. With SeV 50-75% of the M protein was seen in the nucleus compared to 30% with the wild-type SeV M protein (48). Overall, with some paramyxoviruses it has been shown that if you have either the NLS mutated and a functional NES or if you have the NES mutated and a functional NLS nuclear exclusion or retention is seen, showing that both domains are essential for normal nuclear transit.

The mutant L106/107A was not detected in cell lysates through the standard western blot procedure (Figure 11 Lane 5). Because we were not able to see expression with the L106/107A mutant in the lysate samples we could not determine if this mutation had an impact on budding. Because the L106/107A mutant was detected at similar levels to the wild-type and mutant M proteins with IF assay, the IF procedure was repeated in parallel with the western blot procedure with the same experimental conditions. The L106/107A mutant was detected by IF (as previously seen), but not by western blotting. Since the L106/107A mutant was able to be detected with the immunofluorescence protocol and not the western blot procedure, detection of this mutant with immunofluorescence could be due to the addition of formaldehyde to fix the cells. Formaldehyde has the ability to mutate epitopes, thus it could be possible that the only reason this mutant was seen with immunofluorescence was due to the change in epitopes therefore allowing the antibody to bind to this mutant. To test this a different fixative agent could be used and the mutant could be viewed again with immunofluorescence microscopy to see if it is able to be detected with this method without the addition of formaldehyde. The lack of detection of this mutant with the western blot procedure could be caused by the release of proteolytic enzymes upon cell lysis and consequently the degradation of the protein. This mutant could be more susceptible to degradation because the structure was altered. To test this, addition of protease inhibitors to the cell lysis buffer could be done to see if the L106/107A mutant could be detected through the western blot procedure. Also, lack of detection of the L106/107A mutant could be due to lysis conditions not fully breaking down the membranes of cellular organelles thus not freeing nuclear proteins as well, therefore the L106/107A mutant could be trapped in the

nucleus, which would explain why this mutant could not be detected in the cell lysates. To test this, a higher concentration of cell lysis buffer or addition of SDS to the cell lysis buffer could be tested to ensure nuclear breakdown and release of proteins from inside the nucleus. In contrast to the Hoffman lab Wang *et al.* could express the L106/107A mutant with NiV and showed that this mutation inhibited VLP budding, approximately only 3% could bud compared to 100% for Wild-type M VLP.

Overall, it was found that nuclear transit of the HPIV3 M protein is controlled by NLS and NES domains. The mutation K258A impacted nuclear import and the K258R and L106/107A mutations limited nuclear export. Restricting nuclear entry or limiting nuclear release does not allow for VLP formation, thus, uninhibited travel through the nucleus is needed for budding. To confirm physiological relevance of these observations, the NLS and NES mutants can be inserted into HPIV3 to examine their effects on virus replication. To test physiological relevance Pentecost *et al.* inserted NLS K254R (aligned to HPIV3 K258R) and NES L102/103A (aligned to HPIV3 L106/107A) mutations into recombinant T7-driven SeV and examined their impact on the virus. Specifically, they observed that both wild-type and mutant SeV could be rescued at similar levels, but only wild-type SeV produced infectious viral titers (10^7 I.U./ml). The mutants did not produce detectible infectious viral titers (< 10 I.U./ml; 48). Because of the relatedness between SeV and HPIV3 it is likely that these mutations will impact HPIV3 in the same manner.

REFERENCES

1. Feldmann H, Sanchez A, Heisbert TW. 2013. Chapter 32: *Filoviridae*: Marburg and Ebola viruses, pp. 923-956. In: Fields Virology, 6th ed., vol. 1, Philadelphia, PA.

2. Lyles DS, Kuzmin IV, Rupprecht CE. 2013. Chapter 31: *Rhabdoviridae*, pp. 885-992. In: Fields Virology, 6th ed., vol. 1, Philadelphia, PA.

3. Lamb RA, Parks GD. 2013. Chapter 33: *Paramyxoviridae*, pp. 957-995. In: Fields Virology, 6th ed., vol. 1, Philadelphia, PA.

4. Karron RA, Collins PL. 2013. Chapter 34: Parainfluenza viruses. In: Fields Virology, 6th ed., vol. 1, Philadelphia, PA.

5. Alayyoubie M, Leser GP, Kors CA, Lamb RA. 2015. Structure of the paramyxovirus parainfluenza virus 5 nucleoprotein-RNA complex. Proc Natl Acad Sci USA 112:1792-1799.

6. Wang L, Mackenzie JS, Broder CC. 2013. Chapter 37: Henipaviruses, pp. 1070-1085. In: Fields Virology, 6th ed., vol. 1, Philadelphia, PA.

7. Kirchhoff J, Uhlenbruck S, Goris K, Keil GM, Herrler G. 2014. Three viruses of the bovine respiratory disease complex apply different strategies to initiate infection. Vet Res 45:20.

8. Slobod KS, Shenep JL, Luján-Zilbermann J, Allison K, Brown B, Scroggs RA, Portner A, Coleclough C, Hurwitz JL. 2004. Safety and immunogenicity of intranasal murine parainfluenza virus type I (Sendai virus) in healthy human adults. Vaccine 22:3182-3186.

9. Russel R, Paterson RG, Lamb RA. 1994. Studies with cross-linking reagents on the oligomeric form of the paramyxovirus fusion protein. Virology 199:160-168.

10. Durbin AP, Karron RA. 2003. Progress in the Development of Respiratory Syncytial Virus and Parainfluenza Virus. Vaccines 37.

11. Henrickson KJ. 2003. Parainfluenza Viruses. Clinical Microbiology Reviews 16:242-264.

12. Schomacker H, Schaap-Nutt A, Collins PL, Schmidt AC. 2012. Pathogenesis of acute respiratory illness caused by human parainfluenza viruses. Curr Opin Virol 2:294-299.

13. Bjornson C, Russell KF, Vandermeer B, Durec T, Klassen TP, Johnson DW. 2011. Nebulized epinephrine for croup in children. Cochrane Database Sys Rev CD006619.

14. Ausejo M, Saenz A, Pham B, Kellner JD, Johnson DW, Moher D, Klassen TP. 1993. The effectiveness of glucocorticoids in treating croup: meta-analysis. BMJ 319:5950600.

15. Johnson DW, Jacobson S, Edney PC, Hadfield P, Mundy ME, Schuh S. 1998. A comparison of nebulized budesonide, intramuscular dexamethasone, and placebo for moderately severe croup. N Engl J Med 339:498-503.

16. Glezen WP, Frank AL, Taber LH, Kasel JA. 1984. Parainfluenza virus type 3: seasonality and risk of infections and reinfection in young children. J Infect Dis 150:851-857.

17. Denny FW, Clyde WA. 1986. Acute lower respiratory tract infections in nonhospitalized children. J Pediatr 108:635-646.

18. Shay DK, Holman RC, Newman RD, Liu LL, Stout JW, Anderson LJ. 1999. Bronchiolitis-associated hospitalization amoung US children, 1980-1996. JAMA 282:14401446.

19. Cooney MK, Fox JP, Hall CE. The Seattle Virus Watch. VI. Observations of infections with and illness due to parainfluenza, mumps and respiratory syncytial virus and Mycoplasma pneumoniae. 1975. Am J Epidemiol 101: 532-51.

20. Mao H, Thakur CS, Chattopadhay S, Silverman RH, Gudkov A, Banerjee AK. 2008. Inhibition of human parainfluenza virus type 3 infection by novel small molecules. Antiviral Res 77:83-94.

21. Moscona A. 2005. Entry of parainfluenza virus into cells as a target for interrupting childhood respiratory disease. J Clin Invest 115:1688-1698.

22. Hsu M, Scheid A, Choppin AS. 1979. Reconstitution of membranes with individual paramyxovirus glycoproteins and phospholipid in cholate solution. Virology 95:476-491.

23. Zhang G, Zhang S, Ding B, Yang X, Chen L, Yan Q, Jiang Y, Zhong Y, Chen M. 2014. A leucine residue in the C terminus of human parainfluenza virus type 3 matrix protein is essential for efficient virus-like particle and virion release. J Virol 88:13173-13188.

24. Malur AG, Chattopadhyay S, Maitra RK, Banerjee AK. 2005. Inhibition of STAT 1 phosphorylation by human parainfluenza virus type 3 C protein. J Virol 79:7877-7882.

25. Caignard G, Komarova AV, Bouraï M, Mourez T, Jacob Y, Jones LM, Rozenberg F, Vabret A, Freymuth F, Tangy F, Vidalain PO. 2009. Differential regulation of type I interferon and epidermal growth factor pathways by a human Respirovirus virulence factor. PLoS Pathog 5:e100587.

26. Malur AG, Hoffman MA, Banerjee AK. 2004. The human parainfluenza virus type 3 (HPIV 3) C protein inhibits viral transcription. Virus Res 99:199-204.

27. Huberman K, Peluso R, Moscona A. 1995. The hemagglutinin-neuraminidase of human parainfluenza virus type 3: role of the neuraminidase in the viral life cycle. Virology 214:294-303.

28. Porotto M, Greengard O, Poltoratskaia N, Horga MA, Moscona A. 2001. Human parainfluenza virus type 3 HN-receptor interaction: the effect of 4-GU-DANA on a neuraminidase-deficient variant. J Virology 76:7481-7488.

29. Pantua HD, McGinnes LW, Peeples ME, Morrison TG. 2006. Requirements for the assembly and release of Newcastle disease virus-like particles. Journal of virology 80:11062–73.

30. Luo L, Li Y, Kang CY. 1990. Expression of gag precursor protein and secretion of virus-like gag particles of HIV-2 from recombinant baculovirus-infected cells. Virology 179:874-880.

31. Li Y, Luo L, Schubert M, Wagner RR, Kang CY. 1993. Viral liposomes released from insect cells infected with recombinant baculovirus expressing the matrix protein of vesicular stomatitis virus. J Virol 67:4415-4420.

32. Gonzalez S, Affranchino JL, Gelderblom HR, Burny A. 1993. Assembly of the matrix protein of simian immunodeficiency virus into virus-like particles. Virology 194:548-556.

33. Gheysen D, Jacobs E, de Foresta F, Thiriart C, Francotte M, Thines D, De Wilde M. 1989. Assembly and release of HIV-1 precursor Pr55gag virus-like particles from recombinant baculovirus-infected insect cells. Cell 59:103-112.

34. Delchambre M, Gheysen D, Thines D, Thiriart C, Jacobs E, Verdin E, Horth M, Burny A, Bex F. 1989. The GAG precursor of simian immunodeficiency virus assembles into virus-like particles. EMBO J 8:2653-2660.

35. Timmins J, Scianimanico S, Schoehn G, Weissenhorn W. 2001. Vesicular release of Ebola virus matrix protein VP40. Virology 283:1-6.

36. Jasenosky LD, Neumann G, Lukashevich I, Kawaoka Y. 2001. Ebola virus VP40-induced particle formation and association with lipid bilayer. J Virol 75:5205-5214.

37. Coronel EC, Murti GK, Takimoto T, Portner A. 1999. Human parainfluenza virus type 1 matrix and nucleoprotein genes transiently expressed in mammalian cells induce the release of virus-like particles containing nucleocapsid-like structures. J Virol 73:7035-7038.

38. Sugahara F, Uchiyama T, Watanabe H, Shimazu Y, Kuwayama M, Fujii Y, Kiyotani K, Adachi A, Kohno N, Yoshida T, Sakaguchi T. 2004. Paramyxovirus Sendai virus-like particle formation by expression of multiple viral proteins and acceleration of its release by C protein. Virology 325:1-10.

39. Runkler N, Pohl C, Schneider-Schaulies S, Klenk HD, Maisner A. 2007. Measles virus nucleocapsid transport to the plasma membrane requires stable expression and surface accumulation of the viral matrix protein. Cell Microbiol 9:1203-1214.

40. Patch JR, Crameri G, Wang LF, Eaton BT, Broder CC. 2007. Quantitative analysis of Nipah virus proteins released as virus-like particles reveals central role for the matrix protein. Virol J 4:1.

41. Li D, Jans DA, Bardin PG, Meanger J, Mills J, Ghildyal R. 2008. Association of respiratory syncytial virus M protein with viral nucleocapsids is mediated by the M2-1 protein. J Virol 82:8863-8870.

42. Bracken M, Hayes B, Kandel S, Scott-Shemon D, Ackerson L, Hoffman M. 2016. Viral protein requirements for assembly and release human parainfluenza virus type 3 virus-like particles. Journal of General Virology 97: 1-6.

43. Li M, Schmitt PT, Li Z, McCrory TS, He B. 2009. Mumps virus matrix, fusion, and nucleocapsid proteins cooperate for efficient production of virus-like particles. J Virol 83:7261-7272.

44. Schmitt AP, Leser GP, Waning DL, Lamb RA. 2002. Requirements for budding of paramyxovirus simian virus 5 virus-like particles. J Virol 76:3952-3964.

45. Wollert T, Hurley JH. 2010. Molecular mechanism of multivesicular body biogenesis by ESCRT complexes. Nature 464:864–9.

46. Göttlinger HG, Dorfman T, Sodroski JG, Haseltine WA. 1991. Effect of mutations affecting the p6 gag protein on human immunodeficiency virus particle release. Pro Natl Acad Sci USA 88:3195-3199.

47. Bieniasz PD. 2006. Late budding domains and host proteins in enveloped virus release. Virology 344:55-63.

48. Pentecost M, Vashisht AA, Lester T, Voros T, Beaty SM, Park A, Wang YE, Yun TE, Freiberg AN, Wohlschlegel JA, Lee B. 2015. Evidence for ubiquitin-regulated nuclear and subnuclear trafficking among *Paramyxovirinae* matrix proteins. PLOS Path 11:e1004739.

49. Wang YE, Park A, Lake M, Pentecost M, Torres B, Yun TE, Wold MC, Holbrook MR, Freiberg AN, Lee B. 2010. Ubiquitin-regulated nuclear-cytoplasmic trafficking of the Nipah virus matrix protein is important for viral budding. PLoSPathog 6: e1001186.

50. Martin-serrano J, Eastman SW, Chung W, Bieniasz PD. 2005. Motifs to the vacuolar protein-sorting pathway. Cell Biol 168:89–101.

51. Chen BJ, Lamb RA. 2008. Mechanisms for enveloped virus budding: can some viruses do without an ESCRT? Virology 372:221–32.

52. Calistri A, Salata C, Parolin C, Palù G. 2009. Role of multivesicular bodies and their components in the egress of enveloped RNA viruses. Reviews in Medical Virology 19:31–45.

53. Bissig C, Lenoir M, Velluz M-C, Kufareva I, Abagyan R, Overduin M, Gruenberg J. 2013. Viral infection controlled by a calcium-dependent lipid-binding module in Alix. Developmental cell 25:364–73.

54. Yarbrough ML, Mata MA, Sakthive lR, Fontoura BM. 2014. Viral subversion of nucleocytoplasmic trafficking. Traffic 15:127–140.

55. Scott MS, Troshin PV, Barton GJ. 2011. Nucleolar localization sequence detect or for eukaryotic and viral proteins. BMC Bioinformatics 12:317.

56. Railborg C, Stenmark H. 2009. The ESCRT machinery in endosomal sorting of ubiquitylated membrane proteins. Nature 458:445-452.

57. Hurley JH, Emr SD. 2006. The ESCRT complexes: structure and mechanism of a membrane-trafficking network. Annu Rev Biophys Biomol Struct 35:277-298.

58. Saksena S, Emr SD. 2009. ESCRTs and human disease. Biochemical Society transactions 37:167–72.

59. Spriggs MK, Johnson PR, Collins PL. 1987. Sequence analysis of the matrix protein gene of human parainfluenza virus type 3: extensive sequence homology among paramyxoviruses. J Gen Virol 68:1491-1497.

60. Galinski MS, Mink MA, Lambert DM, Wechsler SL, Pons MW. 1987. Molecular cloning and sequence analysis of the human parainfluenza 3 virus gene encoding the matrix protein. Virology 157:24-30.

61. Luk D, Masters PS, Sánchez A, Banerjee AK. 1987. Complete nucleotide sequence of the matri protein mRNA and three intergenic junctions of human parainfluenza virus type 3. Virology 156:189-192.

62. Komander D, Rape M. 2012. The ubiquitin code. AnnuRevBiochem 81:203–229.

63. Shields SB, Piper RC. 2011. How ubiquitin functions with ESCRTs. Traffic 12:1306–1317.

64. Votteler J, Sundquist WI. 2013. Virus budding and the ESCRT pathway. Cell Host Microbe 14: 232–241.

65. Prinoski K, Cote MJ, Kang CY, Dimock K. 1987. Nucleotide sequence of the human parainfluenza virus 3 matrix protein gene. Nucleic Acids Res 15:3182.